INL/RPT-22-69883
Revision 0

Development of Temperature Compensation Tools for SPNDs Operating in High Temperature Environments

October 2022

Milestone Report—M3CT-22IN0702014

Kevin Tsai
Idaho National Laboratory

Idaho National Laboratory

INL is a U.S. Department of Energy National Laboratory
operated by Battelle Energy Alliance, LLC

INL/RPT-22-69883
Revision 0

Development of Temperature Compensation Tools for SPNDs Operating in High Temperature Environments

Milestone Report—M3CT-22IN0702014

Kevin Tsai
Idaho National Laboratory

October 2022

Idaho National Laboratory
Idaho Falls, Idaho 83415

http://www.inl.gov

Prepared for the
U.S. Department of Energy
Office of Nuclear Energy
Under DOE Idaho Operations Office
Contract DE-AC07-05ID14517

Page intentionally left blank

ABSTRACT

Two rhodium-based self-powered neutron detectors (Rh-SPNDs) were irradiated at the Massachusetts Institute of Technology Reactor as a follow-on experiment to the heated irradiation previously conducted at the Neutron Radiography facility at Idaho National Laboratory. The experiment was conducted over the temperature ranges of 600-850°C to further examine the effects of temperature on the Rh-SPNDs. Four tests of varying temperature and power were performed. The tests identified two types of temperature effects consistent with historical evaluations. One effect is a prompt proportionality to temperature at steady-state reactor power due to the decrease in Rh-SPND insulation resistance. The other effect is a delayed effect generated from displacement currents generated by changing the space charge within the insulator as a function of temperature.

The result of this experiment demonstrates a characterizable responses to temperature that shows feasibility for developing a temperature compensation tool for SPNDs operating in high temperatures. The characteristics identified in this experiment will be integrated within the delayed-response compensation techniques for a fiscal year 2023 (FY-23) evaluation.

Page intentionally left blank

ACKNOWLEDGEMENTS

The authors would like to thank these people for their significant contributions to the success of this work: Ashley Lambson for the fabrication support; Lisa Moore-McAteer, Kort Bowman, and Troy Unruh for procurement and logistics, Joe Palmer for experiment management; and the MIT-NRL staff, David Carpenter, Michael Ames, and Yakov Ostrovsky, for experiment assembly and measurement support.

Page intentionally left blank

CONTENTS

FIGURES

TABLES

Page intentionally left blank

ACRONYMS

INL	Idaho National Laboratory
MITR	Massachusetts Institute of Technology Reactor
NRAD	Neutron Radiography Facility
NSUF	Nuclear Science User Facility
Rh-SPND	Rhodium-based self-powered neutron detector
SPND	Self-powered neutron detector

Page intentionally left blank

Development of Temperature Compensation Tools for SPNDs Operating in High Temperature Environments

1. INTRODUCTION

This report documents the research toward developing a temperature compensation tool for self-powered neutron detectors (SPNDs) operating in high-temperature environments. The data used to develop the compensation tool is derived from the initial assessment in [1] and the follow-on irradiation, funded in collaboration with the Nuclear Science User Facility (NSUF), conducted at the Massachusetts Institute of Technology Reactor (MITR) which is discussed in later sections.

The SPNDs used in this irradiation are the same rhodium-based SPNDs (Rh-SPNDs) from the assessments performed at the Neutron Radiography (NRAD) facility at Idaho National Laboratory (INL) [1]. These Rh-SPNDs have demonstrated the potential for advanced reactor applications—operability up to 500°C and survivability in temperatures up to 850°C. Performance beyond 500°C was concluded to be temporarily but significantly affected by the electrically driven heater power supply. However, operability was still observed after the SPND signals reached a stability point after the heater power supply effects subsided. This was the primary motivation in performing follow-on testing at MITR, which uses gamma heating within a tungsten rod as the heater.

1.1 Rh-SPND Overview

As discussed, the two Rh-SPNDs deployed at MITR are the exact same SPNDs previously tested at NRAD [1]. Relevant geometries of the two SPNDs are given in Table 1. In the simplest form of operation, Rh-SPNDs generate their electric signal through neutron activation and subsequent beta-particle decay, an (n, β) reaction, within the rhodium emitter. The generation of SPND signal therefore does not require application of voltage potential. However, the detector is considered a delayed-response SPND governed by the decay time constants of the reaction. In the case of the Rh-SPND, the beta-decay constants are from isotopes Rh-104 and Rh-104m which have respective thermal neutron activation cross-sections of 139 b and 11 b, with half-lives of 44 s and 265 s [2].

The advantage of directly measuring the electric current from the beta-decay of the Rh-SPND is that the saturated signal is largely proportional to the steady-state neutron flux at the emitter. The disadvantage of measuring the beta-decay signal is the delayed-response of the signal in a dynamic neutron field as it would require signal compensation techniques to derive the prompt changes in neutron flux. Due to these conditions, Rh-SPNDs are most often used for core flux mapping during steady-state operations rather than reactor safety and control. However, the delayed-response compensation methods such as direct inversion and Kalman filters have been extensively researched to improve the response time to demonstrate the potential for reactor safety and control use [3], [4], [5].

While typical application of the SPNDs is primarily in light water reactors, few studies evaluate sensor performance in high temperatures. Detector resistance, signals, and leakage current within a TRIGA ® reactor with experimental temperatures up to 800°C were measured [6] and demonstrated reproducible non-linear irregularities among the three detectors depending on which parameter—temperature or neutron flux—is varied. Measurements on electric conductivity of Rh- and Pt-SPNDs showed an approach to the properties of the mineral-insulated cable starting around 300°C [7]. Investigations on a sharp signal rise, followed by a relaxation to steady-state value during heating from 300–700°C was performed by Mitel'man [8]. A proposed explanation for the sharp signal rise was the displacement current generated from a change in the space charge of the insulator as a function of temperature.

Table 1. Rh-SPND material and geometry overview.

SPND Design	Emitter	Insulator at Emitter Region	Sheath
Large Rh-SPND	Rhodium	Al_2O_3	I-600
(ILC-102-RhSPND)	0.032 in. OD	0.072 in. OD	0.102 in. OD
	3.50 in. L	0.032 in. ID	0.072 in. ID
Small Rh-SPND	Rhodium	MgO	I-600
(ILC-080-RhSPND)	0.020 in. OD	0.056 in. OD	0.080 in. OD
	3.50 in. L	0.020 in. ID	0.056 in. ID

1.2 MITR Experimental Overview

The MITR irradiation is carried out in a 2" outer diameter (OD) dry tube in the A-1 position of the MITR core given in Figure 1. The experiment capsule is a titanium capsule containing a graphite holder with sensor inserts around a central tungsten rod (Figure 2). The capsule's temperature is controlled through gamma heating of the tungsten rod and varying the gas-flow composition between helium and neon through the capsule to decrease or increase temperature. The minimum achievable temperature, at reactor full power with maximum helium flow, is around 600°C. The maximum achievable temperature, at reactor full power and maximum neon flow, is roughly 800°C. Four types of tests were performed:

Test 1. Max reactor power and linear increase to temperature.

Test 2. Max reactor power and stepwise increase to temperature.

Test 3. Max reactor power and stepwise increase and stepwise decrease to temperature.

Test 4. Maintain temperature and stepwise decrease power.

The emitter and compensator signals of both Rh-SPNDs are measured by two Keithley dual-channel electrometers (Keithley 6482) and were recorded via a Nuclear Instruments CompactDAQ system with LabVIEW interface.

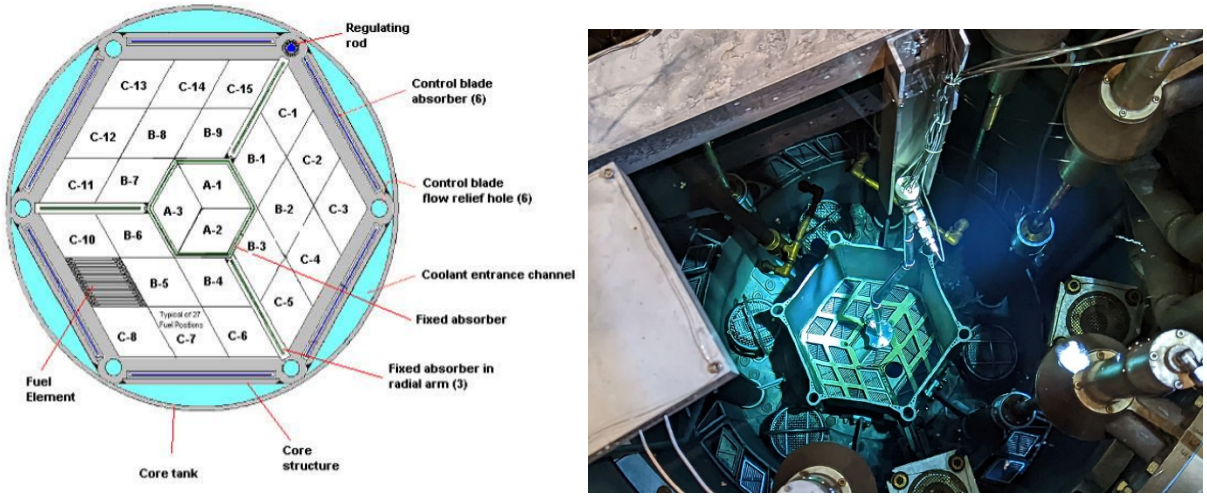

Figure 1. (Left) MITR core map overview. Image taken from [9]. (Right) Picture of the SPND experiment.

Figure 2. MITR capsule assembly with the tungsten alloy rod in the center position surrounded by sensors.

2. RESULTS

2.1 Test 1 Results

Test 1 is to hold at maximum power (5.7 MW) and allow the temperature to linearly increase from 580 to 600°C naturally without changing gas composition (100% helium flow).

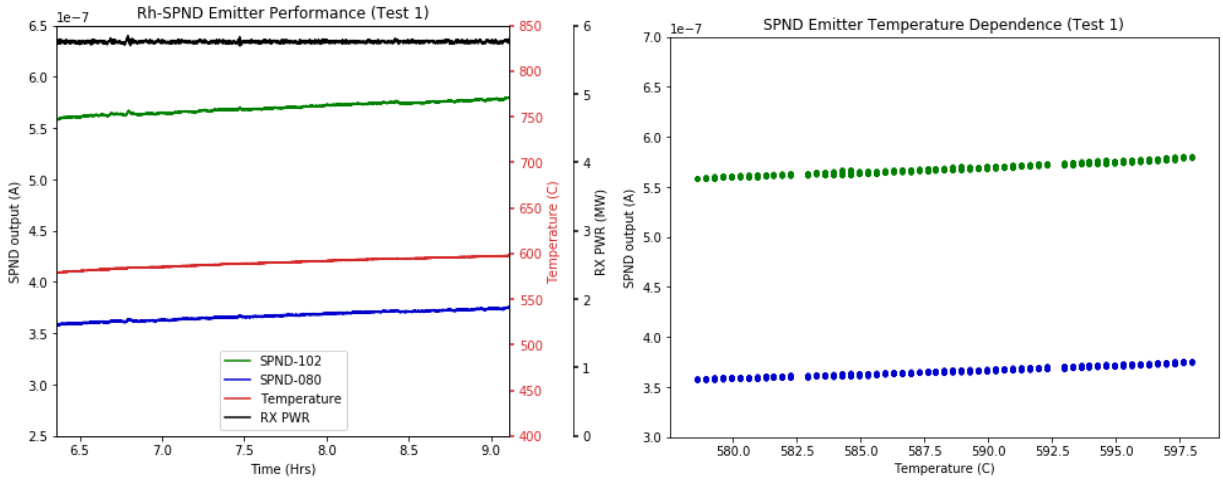

Figure 3. (Left) SPND signal as a function of time during linear heat-up. (Right) SPND signal as a function of temperature.

The plots in Figure 3 shows the linear relationship between the SPND emitter signal and the temperature. Performing a linear regression, the relationship is given by:

2.2 Test 2 Results

Test 2 is to maintain maximum power (5.7 MW) and stepwise increase the temperature to a final point. This test is accomplished by increasing the amount of neon in the flow-gas composition. Temperatures within this test range from 600 to 750°C. The evaluations of temperature effects on the SPND signals are split into two regions: stepwise increase from 600 to 750°C and maintaining 750°C over time.

In the same process as Test 1, the SPNDs' temperature dependence with stepwise temperature increase are plotted in Figure 4. The regression equations given below continues to show a linear dependence for ILC-102-Rh-SPND; however, ILC-080-Rh-SPND began to demonstrate non-linear (or nearly temperature independent) behavior as given by the r^2 value of the regression.

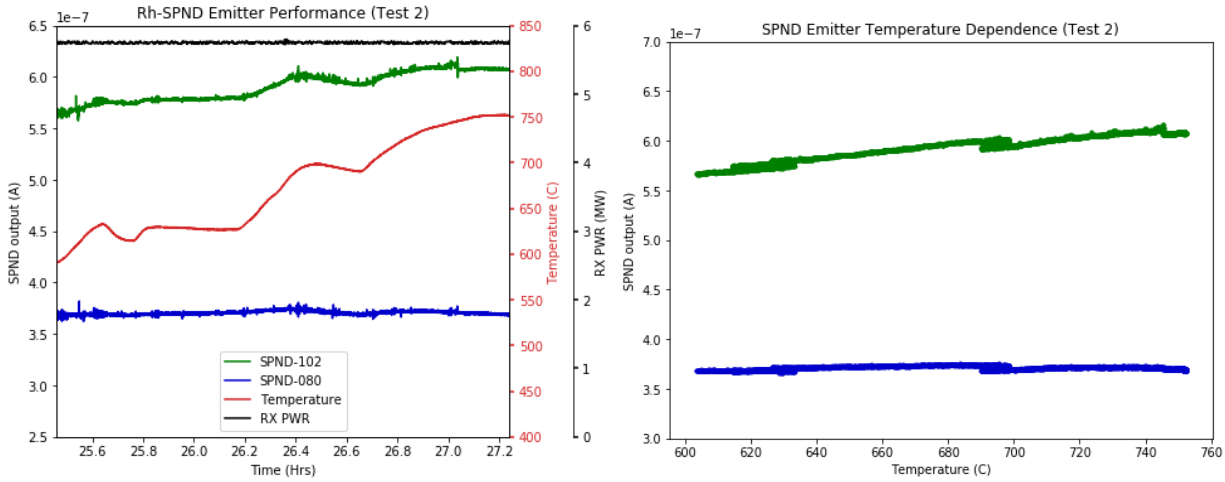

Figure 4. SPND signal as a function of time during stepwise heat-up. (Right) SPND signal as a function of temperature.

Figure 5 shows the plot of SPND signals at 750°C (with only 5°C of drop over time). The ILC-102-Rh-SPND continues to show a linear relationship to the small variation in temperature. Meanwhile, ILC-080-Rh-SPND continues to demonstrate a non-linear (or nearly temperature independent) behavior as given by their regression below:

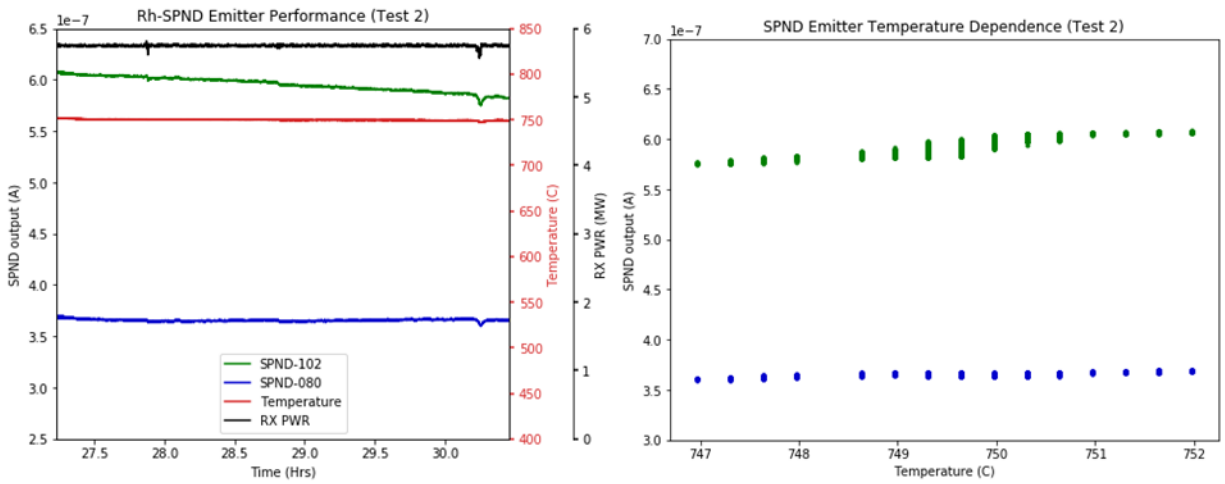

Figure 5. SPND signal as a function of time during steady temperature of 750°C. (Right) SPND signal as a function of temperature.

2.3 Test 3 Results

Test 3 is to identify SPND signal invertibility through a series of stepwise temperature increase from 600 to 820°C followed by stepwise temperature decreases back to 600°C. As depicted in Figure 6, a non-invertible response to temperature is identified. A cause for the non-invertible curve is observed at the maximum temperature plateau. At maximum temperature the reactor had a slight decrease in power. This decrease in power is also observed in the Rh-SPNDs. However, the decrease in signal is not characteristic of Rh-SPND. The decrease in signal is more than expected as a response to power. Regression of the signal versus temperature curves of two regions are performed (peak temperature plateau region is not included):

1. From initial to peak temperature

2. From peak temperature to final temperature

From the slope of the regression performed, it is observed that without the significant decrease at the maximum temperature plateau, ILC-080-Rh-SPND was invertible with temperature ramps while ILC-102-Rh-SPND displayed a more significant drop in signal in response to temperature decrease.

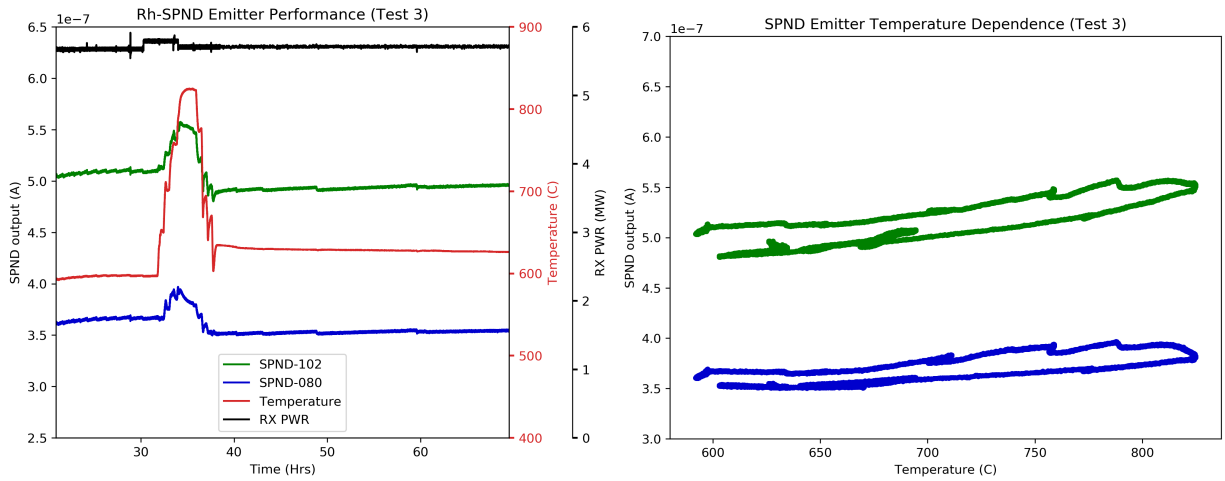

Figure 6. SPND signal as a function of time during stepwise temperature increase and decrease. (Right) SPND signal as a function of temperature.

2.4 Test 4 Results

Test 4 is meant to investigate the capability of Rh-SPNDs to accurately track reactor power at temperature. To perform this test, the temperature was raised to 750°C and maintained for signal stability. At each down-power step of the reactor, the gas-flow system will attempt to increase neon flow to maintain temperature. As shown in Figure 7, the gas-flow system can only maintain temperature for four power steps before the heating becomes insufficient with maximum neon flow. Average reactor power and corresponding SPND signals from all four steps are given in Table 2. Comparison of difference between maximum power and each subsequent power step is given in Table 3.

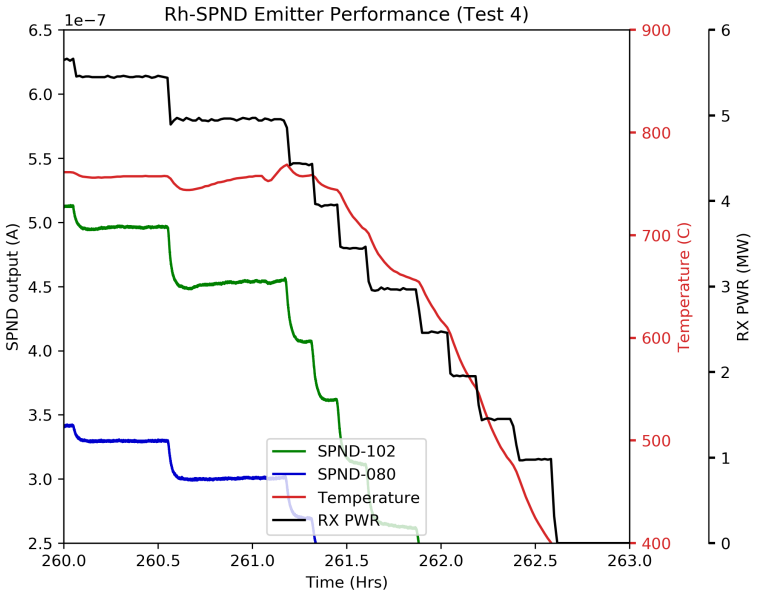

Figure 7 SPND signal as a function of time during power decrease at steady temperature.

Table 2. Reactor power levels and associated Rh-SPND signals.

	RX Power (MW)	ILC-102-RhSPND 102 (A)	ILC-080-RhSPND (A)
Power 1	5.65	5.13E-07	3.42E-07
Power 2	5.45	4.96E-07	3.30E-07
Power 3	4.95	4.53E-07	3.00E-07
Power 4	4.43	4.17E-07	2.76E-07

Table 3. Relative differences of power levels and corresponding SPND signal differences.

Power Difference	RX Power	ILC-102-RhSPND	ILC-080-RhSPND
1 to 2	−0.036	−0.033	−0.035
1 to 3	−0.124	−0.117	−0.121
1 to 4	−0.216	−0.188	−0.193

3. DISCUSSION OF RESULTS

Two Rh-SPNDs were tested at MITR for the purpose of characterizing sensor behavior as a function of temperature. The two SPNDs differ per geometry and insulation material given in Table 1. Overall, the observed effects of temperature on SPNDs are separated into two categories:

1. Signal increase that can be approximated to be linearly proportional with temperature increase.
2. Signal overshoot or undershoot beyond the linear proportionality followed by a slow recovery to stability.

Behavior 1 can be observed in tests 1–3 with the ILC-102-RhSPND displaying a larger response to temperature. The mechanisms to the behavior can be explained by the change in resistance of the insulation properties as a function of temperature noted by Bock [7]. This effect is a prompt response with temperature changes. Additionally, within the temperature ranges of this test, it may be approximated linearly. However, this property is specific to each SPND design. Therefore, resistance characteristics in temperature needs to be performed on a specific design or individual sensor basis to directly compensate for this effect.

Behavior 2 was identified in the steady-temperature range of Test 2 and the temperature plateau of Test 3. The signal overshoot/undershoot behavior was also a characteristic observed during prior testing [1] and historically when operating beyond 300°C [6], [8]. The proposed theory for this mechanism is explained by Mitel'man [8] as a displacement current caused by changes in the space charge of the insulation that was described by Warren [10]. This characteristic was described by Mitel'man [8] to have a larger effect in both the overshoot as well as recovery time-constant in sensors with higher dielectric thickness and higher linear attenuation coefficient for beta-particles. ILC-102-RhSPND was able to demonstrate this theory by both satisfying the two parameters given by Mitel'man [8] over the ILC-080-RhSPND (a thicker Al_2O_3 insulation over a thinner MgO insulation) as well as having observably more effects due to temperature changes across all tests.

This report demonstrates the effects of temperature on the operation of SPNDs from 600 to 850°C. The measurements confirms the behaviors identified historically and provides prompt (behavior 1) and delayed (behavior 2) characteristics that are feasible to integrate within the available response compensation methods evaluated previously [3], [4], [5]. The developed compensation method will be the subject of testing in FY-23.

4. REFERENCES

[1] INL/EXT-21-65635, "Comparative Assessment of Neutron Flux Sensor Technologies for Advanced Reactors," 2021. https://www.osti.gov/servlets/purl/1844428.

[2] G. F. Knoll, Radiation Detection and Measurement, 4th Edition ed., Hoboken: John Wiley and Sons, Inc., 2010.

[3] L. A. Banda and B. I. Nappi, "Dynamic compensation of rhodium self powered neutron detectors," *IEEE Transactions on Nuclear Science,* Vols. NS-23, no. 1, pp. 311-316, 1976.

[4] M. L. Kantrowitz, "An improved dynamic compensation algorithm for rhodium self-powered neutron detectors," *IEEE Transactions on Nuclear Science,* Vols. NS-34, no. 1, pp. 562-566, 1987.

[5] F. Khoshahval, P. Zhang and D. Lee, "Analysis and comparison of direct inversion and Kalman filter methods for self-powered neutron detector compensation," *Nuclear Instruments and Methods in Physics Research Section A: Accelerators, Spectrometers, Detectors and Associated Equipment,* vol. 969, 2020.

[6] J. Ziebermayr and H. Bock, "High temperature incore tests of self-powered neutron detectors," in *INIS-AT--09N002*, Austria, 1976.

[7] H. Bock and J. Rantanen, "Temperature and radiation tests with Pt- and Rh-self-powered neutron detectors," *Nuclear Instruments and Methods,* vol. 164, pp. 205-207, 1979.

[8] M. G. Mitel'man, A. A. Kononovich, V. M. Osipov and N. D. Rozenblyum, "Effect of temperature on characteristic of self-powered detectors," *At Energy,* vol. 48, no. 4, pp. 263-266, 1980.

[9] D. Carpenter, G. Kohse and L. Hu, "MITR users' guide," July 2012. [Online]. Available: https://nrl.mit.edu/sites/default/files/documents/MITR_User_Guide.pdf.

[10] H. D. Warren, "Calculation Model for Self-Powered Neutron Detector," *Nuclear Science and Engineering,* vol. 48, pp. 331-342, 1972.